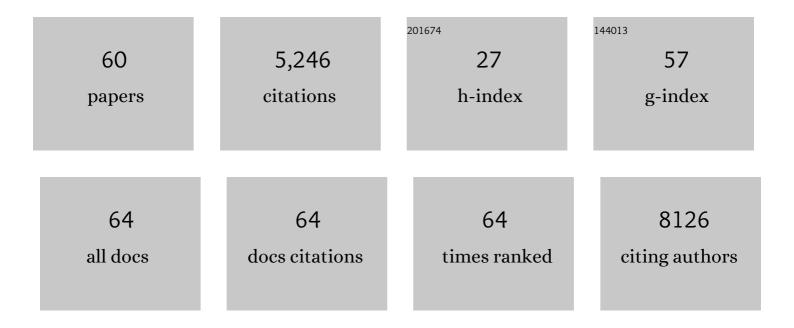
## List of Publications by Year in descending order

Source: https://exaly.com/author-pdf/3422804/publications.pdf Version: 2024-02-01



Сомсти

#	Article	IF	CITATIONS
1	Operando HERFD-XANES and surface sensitive Δμ analyses identify the structural evolution of copper(II) phthalocyanine for electroreduction of CO2. Journal of Energy Chemistry, 2022, 64, 1-7.	12.9	27
2	Approaching theoretical specific capacity of iron-rich lithium iron silicate using graphene-incorporation and fluorine-doping. Journal of Materials Chemistry A, 2022, 10, 4006-4014.	10.3	10
3	Tale of Three Molecular Nitrides: Mononuclear Vanadium (V) and (IV) Nitrides As Well As a Mixed-Valence Trivanadium Nitride Having a V <sub>3</sub> N <sub>4</sub> Double-Diamond Core. Journal of the American Chemical Society, 2022, 144, 10201-10219.	13.7	3
4	Integrated Experimental and Computational K-Edge X-ray Absorption Near-Edge Structure Analysis of Vanadium Catalysts. Journal of Physical Chemistry C, 2022, 126, 11949-11962.	3.1	7
5	The electrolyte comprising more robust water and superhalides transforms Znâ€metal anode reversiblyÂand dendriteâ€free. , 2021, 3, 339-348.		100
6	Thermal Atomic Layer Deposition of Gold: Mechanistic Insights, Nucleation, and Epitaxy. ACS Applied Materials & Interfaces, 2021, 13, 9091-9100.	8.0	2
7	Computational Investigation of the Role of Active Site Heterogeneity for a Supported Organovanadium(III) Hydrogenation Catalyst. ACS Catalysis, 2021, 11, 7257-7269.	11.2	16
8	Single-Molecule Kinetics of Styrene Hydrogenation on Silica-Supported Vanadium: The Role of Disorder for Single-Atom Catalysts. Journal of Physical Chemistry C, 2021, 125, 20286-20300.	3.1	10
9	Role of Boron in Enhancing the Catalytic Performance of Supported Platinum Catalysts for the Nonoxidative Dehydrogenation of <i>n</i> Butane. ACS Catalysis, 2020, 10, 1500-1510.	11.2	21
10	Cation Additive Enabled Rechargeable LiOHâ€Based Lithium–Oxygen Batteries. Angewandte Chemie - International Edition, 2020, 59, 22978-22982.	13.8	29
11	Revealing nanoscale mineralization pathways of hydroxyapatite using in situ liquid cell transmission electron microscopy. Science Advances, 2020, 6, .	10.3	61
12	Electrochemical Investigation of Low-Valent Multiply M≡M Bonded Group VI Dimers: A Standard Chemical Reduction Leads to an Unexpected Product. Organometallics, 2020, 39, 4430-4436.	2.3	6
13	Highly selective electrocatalytic CO2 reduction to ethanol by metallic clusters dynamically formed from atomically dispersed copper. Nature Energy, 2020, 5, 623-632.	39.5	393
14	Titelbild: Cation Additive Enabled Rechargeable LiOHâ€Based Lithium–Oxygen Batteries (Angew. Chem.) Tj ETG	Qq <u>Q</u> 80 rg	;BT <sub>d</sub> Overlock
15	Cation Additive Enabled Rechargeable LiOHâ€Based Lithium–Oxygen Batteries. Angewandte Chemie, 2020, 132, 23178-23182.	2.0	8
16	Pairwise semi-hydrogenation of alkyne to <i>cis</i> -alkene on platinum-tin intermetallic compounds. Nanoscale, 2020, 12, 8519-8524.	5.6	12
17	Tuning Li <sub>2</sub> O <sub>2</sub> Formation Routes by Facet Engineering of MnO <sub>2</sub> Cathode Catalysts. Journal of the American Chemical Society, 2019, 141, 12832-12838.	13.7	107

18In situ Liquid Cell Transmission Electron Microscopy Study of Hydroxyapatite Mineralization Process.<br/>Microscopy and Microanalysis, 2019, 25, 1502-1502.0.41

#	Article	IF	CITATIONS
19	Mechanistic Aspects of a Surface Organovanadium(III) Catalyst for Hydrocarbon Hydrogenation and Dehydrogenation. ACS Catalysis, 2019, 9, 11055-11066.	11.2	17
20	Theoretical Determination of Size Effects in Zeolite-Catalyzed Alcohol Dehydration. Catalysts, 2019, 9, 700.	3.5	11
21	Highly Efficient Solarâ€Driven Carbon Dioxide Reduction on Molybdenum Disulfide Catalyst Using Choline Chlorideâ€Based Electrolyte. Advanced Energy Materials, 2019, 9, 1803536.	19.5	34
22	Insights into Structural Evolution of Lithium Peroxides with Reduced Charge Overpotential in Liâ^O <sub>2</sub> System. Advanced Energy Materials, 2019, 9, 1900662.	19.5	38
23	Deciphering the Atomic Patterns Leading to MnO2 Polymorphism. CheM, 2019, 5, 1793-1805.	11.7	46
24	Electrophilic Organoiridium(III) Pincer Complexes on Sulfated Zirconia for Hydrocarbon Activation and Functionalization. Journal of the American Chemical Society, 2019, 141, 6325-6337.	13.7	38
25	Enhancing electrocatalysis for hydrogen production over CoP catalyst by strain: a density functional theory study. Physical Chemistry Chemical Physics, 2019, 21, 9137-9140.	2.8	15
26	Facet-dependent active sites of a single Cu2O particle photocatalyst for CO2 reduction to methanol. Nature Energy, 2019, 4, 957-968.	39.5	349
27	Ordering Heterogeneity of [MnO6] Octahedra in Tunnel-Structured MnO2 and Its Influence on Ion Storage. Joule, 2019, 3, 471-484.	24.0	123
28	Hydrogen Activation by Silica-Supported Metal Ion Catalysts: Catalytic Properties of Metals and Performance of DFT Functionals. Journal of Physical Chemistry A, 2019, 123, 171-186.	2.5	3
29	Encapsulating Various Sulfur Allotropes within Graphene Nanocages for Long‣asting Lithium Storage. Advanced Functional Materials, 2018, 28, 1706443.	14.9	60
30	Chemoselective Hydrogenation with Supported Organoplatinum(IV) Catalyst on Zn(II)-Modified Silica. Journal of the American Chemical Society, 2018, 140, 3940-3951.	13.7	56
31	Evidence for Redox Mechanisms in Organometallic Chemisorption and Reactivity on Sulfated Metal Oxides. Journal of the American Chemical Society, 2018, 140, 6308-6316.	13.7	34
32	Water Oxidation Catalysis via Size-Selected Iridium Clusters. Journal of Physical Chemistry C, 2018, 122, 9965-9972.	3.1	20
33	A lithium–oxygen battery with a long cycle life in an air-like atmosphere. Nature, 2018, 555, 502-506.	27.8	433
34	Nuclearity effects in supported, single-site Fe( <scp>ii</scp> ) hydrogenation pre-catalysts. Dalton Transactions, 2018, 47, 10842-10846.	3.3	9
35	Atomically Precise Strategy to a PtZn Alloy Nanocluster Catalyst for the Deep Dehydrogenation of <i>n</i> -Butane to 1,3-Butadiene. ACS Catalysis, 2018, 8, 10058-10063.	11.2	67
36	Development of activity–descriptor relationships for supported metal ion hydrogenation catalysts on silica. Polyhedron, 2018, 152, 73-83.	2.2	11

#	Article	IF	CITATIONS
37	Sub-4 nm PtZn Intermetallic Nanoparticles for Enhanced Mass and Specific Activities in Catalytic Electrooxidation Reaction. Journal of the American Chemical Society, 2017, 139, 4762-4768.	13.7	265
38	Toward Highly Efficient Electrocatalyst for Li–O <sub>2</sub> Batteries Using Biphasic N-Doping Cobalt@Graphene Multiple-Capsule Heterostructures. Nano Letters, 2017, 17, 2959-2966.	9.1	91
39	Copper Cluster Size Effect in Methanol Synthesis from CO <sub>2</sub> . Journal of Physical Chemistry C, 2017, 121, 10406-10412.	3.1	144
40	Isolated, well-defined organovanadium( <scp>iii</scp> ) on silica: single-site catalyst for hydrogenation of alkenes and alkynes. Chemical Communications, 2017, 53, 7325-7328.	4.1	26
41	Burning lithium in CS2 for high-performing compact Li2S–graphene nanocapsules for Li–SÂbatteries. Nature Energy, 2017, 2, .	39.5	349
42	Tailoring the Edge Structure of Molybdenum Disulfide toward Electrocatalytic Reduction of Carbon Dioxide. ACS Nano, 2017, 11, 453-460.	14.6	208
43	Supported Aluminum Catalysts for Olefin Hydrogenation. ACS Catalysis, 2017, 7, 689-694.	11.2	25
44	Nanostructured transition metal dichalcogenide electrocatalysts for CO <sub>2</sub> reduction in ionic liquid. Science, 2016, 353, 467-470.	12.6	778
45	Cathode Based on Molybdenum Disulfide Nanoflakes for Lithium–Oxygen Batteries. ACS Nano, 2016, 10, 2167-2175.	14.6	184
46	Highly Efficient Hydrogen Evolution Reaction Using Crystalline Layered Three-Dimensional Molybdenum Disulfides Grown on Graphene Film. Chemistry of Materials, 2016, 28, 549-555.	6.7	98
47	Cleavage of the βO4 linkage of lignin using group 8 pincer complexes: A DFT study. Journal of Molecular Catalysis A, 2015, 399, 33-41.	4.8	19
48	Carbon Dioxide Conversion to Methanol over Size-Selected Cu <sub>4</sub> Clusters at Low Pressures. Journal of the American Chemical Society, 2015, 137, 8676-8679.	13.7	299
49	Catalytic Upgrading of Biomass-Derived Compounds via C–C Coupling Reactions: Computational and Experimental Studies of Acetaldehyde and Furan Reactions in HZSM-5. Journal of Physical Chemistry C, 2015, 119, 24025-24035.	3.1	19
50	Molecular Dynamics Studies of the Protein–Protein Interactions in Inhibitor of κB Kinase-β. Journal of Chemical Information and Modeling, 2014, 54, 562-572.	5.4	13
51	Computational studies of electrochemical CO <sub>2</sub> reduction on subnanometer transition metal clusters. Physical Chemistry Chemical Physics, 2014, 16, 26584-26599.	2.8	62
52	Investigation of Thermochemistry Associated with the Carbon–Carbon Coupling Reactions of Furan and Furfural Using ab Initio Methods. Journal of Physical Chemistry A, 2014, 118, 4392-4404.	2.5	6
53	Periodic Trends in 3d Metal Mediated CO2 Activation. ACS Symposium Series, 2013, , 67-88.	0.5	3
54	C–O Bond Cleavage of Dimethyl Ether by Transition Metal Ions: A Systematic Study on Catalytic Properties of Metals and Performance of DFT Functionals. Journal of Physical Chemistry A, 2013, 117, 5140-5148.	2.5	26

#	Article	IF	CITATIONS
55	CO <sub>2</sub> Reduction on Transition Metal (Fe, Co, Ni, and Cu) Surfaces: In Comparison with Homogeneous Catalysis. Journal of Physical Chemistry C, 2012, 116, 5681-5688.	3.1	247
56	Reaction Mechanism of the Reverse Water–Cas Shift Reaction Using First-Row Middle Transition Metal Catalysts L′M (M = Fe, Mn, Co): A Computational Study. Inorganic Chemistry, 2011, 50, 8782-8789.	4.0	27
57	Theoretical Studies on the Catalysis of the Reverse Waterâ^Gas Shift Reaction Using First-Row Transition Metal β-Diketiminato Complexes. Journal of Physical Chemistry A, 2010, 114, 6207-6216.	2.5	23
58	Current Development of Pd(II) Complexes as Potential Antitumor Agents. Anti-Cancer Agents in Medicinal Chemistry, 2009, 9, 356-368.	1.7	141
59	Lithium-Ion Battery Materials as Tunable, "Redox Non-Innocent―Catalyst Supports. ACS Catalysis, 0, , 7233-7242.	11.2	6
60	Computational Aspects of Single-Molecule Kinetics for Coupled Catalytic Cycles: A Spectral Analysis. Journal of Physical Chemistry A, 0, , .	2.5	2